Materials Science & Engineering A 631 (2015) 196–200

Contents lists available at ScienceDirect

Materials Science & Engineering A

journal homepage: www.elsevier.com/locate/msea

Hardness–strength relationships in the aluminum alloy 7010

M. Tiryakioğlu [a,*], J.S. Robinson [b], M.A. Salazar-Guapuriche [c], Y.Y. Zhao [d], P.D. Eason [a]

[a] School of Engineering, University of North Florida, Jacksonville, FL 32224, USA
[b] Department of Mechanical, Aeronautical and Biomedical Engineering, University of Limerick, Limerick, Ireland
[c] Materials Laboratory, Airbus UK, Broughton, Chester CH4 0DR, UK
[d] School of Engineering, The University of Liverpool, Liverpool L69 3GH, UK

ARTICLE INFO

Article history:
Received 9 February 2015
Received in revised form
17 February 2015
Accepted 18 February 2015
Available online 26 February 2015

Keywords:
Indentation
Hardness
Tensile testing: constraint factor

ABSTRACT

The relationship between Vickers hardness, yield stress and tensile strength was analyzed by combining data from two independent studies involving 7010 alloy plate and a rectilinear forging. The hardness–yield stress data from the two studies overlapped, suggesting a possible fundamental relationship. Constraint factors calculated by using contact mechanics models were evaluated and the one found by Shaw and DeSalvo was found to agree with the slope for the hardness–yield stress data. The y-intercept of the hardness–yield stress relationship was explained by the work hardening taking place during Vickers testing. The equation found to fit the hardness–yield stress data for 7010 plate and forgings also provided a very respectable fit to a third independent study. Moreover, an empirical equation was developed to express the hardness–tensile strength relationship.

1. Introduction

Wrought Al–Zn–Mg–Cu alloys are used extensively in aerospace applications due to their high strength-to-density ratio (specific strength). Heat treatment of these alloys involves a solution treatment, subsequent quenching, and finally artificial aging that may involve several stages depending on the desired temper. Aluminum alloy 7010 was developed for applications requiring high strength, high fracture toughness, exfoliation resistance and stress corrosion cracking resistance in thick sections [1].

Quality assurance practices in the aerospace industry usually require tensile tests to be conducted on specimens excised from the aluminum parts [2]. Although this practice yields reliable results, excising the tensile coupons not only is time consuming, but also in some applications, leads to the destruction of the part. Therefore, nondestructive methods to estimate the tensile properties, especially yield stress (σ_Y) and tensile strength (S_T), have been of interest to process engineers. One of the most common techniques to estimate yield stress and tensile strength has been hardness testing because of its nondestructive (or semi-destructive) nature, leaving behind only an indentation. Moreover, mechanical data can be gathered quickly without the need for excising samples for testing.

Brinell and Rockwell are among the hardness tests most commonly used in industry. Brinell and most scales in Rockwell use spherical indenters, which yield geometrically dissimilar indentations [3]. Vickers hardness tests use pyramidal indenters, which result in geometrically similar indentations [3]. There have been numerous studies on the geometrical aspects of spherical [3–7] and Vickers [8–10] indentations. In addition, there has been a strong interest in estimating tensile properties from hardness tests. These efforts can be categorized in three groups:

1. Estimating σ_Y and S_T directly from the correlation with hardness [11–14],
2. taking multiple hardness measurements at different loads, calculating mean pressure values and coefficients in given equations which can then be used to estimate σ_Y and S_T [11,15,16],
3. collecting load–indentation depth data throughout the loading and unloading stages of hardness testing, calculating coefficients in a set of equations and using an algorithm to estimate σ_Y and modulus of elasticity, E [8,17].

The present study follows the first method, building on the contact mechanics principles established in the literature. Data from two independent studies, one conducted on a 7010 forging [18] with different quench paths but the same aging treatment, the other [13,19] on 7010 plate with the same quench path but different aging treatments, are combined in the analysis.

* Corresponding author. Tel.: +1 904 620 1390; fax: +1 904 620 1391.
E-mail address: m.tiryakioglu@unf.edu (M. Tiryakioğlu).

http://dx.doi.org/10.1016/j.msea.2015.02.049
0921-5093/

2. Background

The mean pressure under the indenter, P_m, alternatively referred to as the Meyer hardness [20], is found by dividing the load, L, by the projected area of indentation, A_i;

$$P_m = \frac{L}{A_i} \tag{1}$$

The flow stress under the indenter, σ_f, is related to mean pressure;

$$\sigma_f = \frac{P_m}{C} \tag{2}$$

where C is the constraint factor. Hill et al. [21] developed a solution for the stress distribution under a wedge indenter and showed that the pressure normal to the surface of the indenter tip can be found as,

$$P_m = 2\tau_c(1+\theta) \tag{3}$$

where τ_c is the critical maximum shear stress and θ is an angle in the geometric model developed by Hill et al. that is a function of the half angle of the nose of the wedge. For a flat punch, $\theta=\pi/2$. For Vickers indentation, Tabor [3] assumed that the model for a flat punch would be a good approximation. Tabor also used the Huber–Mises criterion, such that,

$$2\tau_c = 1.15\sigma_Y \tag{4}$$

Combining Eqs. (3) and (4) and taking $\theta=\pi/2$, we obtain

$$P_m = 1.15\sigma_Y\left(1+\frac{\pi}{2}\right) \tag{5}$$

Therefore,

$$P_m = 2.956\sigma_Y \tag{5.a}$$

Hence, C is approximately 3 from Eqs. (5.a) and (2) [3], since flow stress is assumed to be equal to yield stress in these loading conditions. Tabor [22] conducted experiments on three fully work-hardened metals, namely tellurium lead, copper and mild steel, and found C to be 2.9, 2.8 and 2.8, respectively. Since Tabor's statement was that $C \approx 3$, many researchers assumed the mean pressure under an indenter to be three times the tensile yield strength of the metal.

In calculating Vickers hardness, H_V[1], load is divided by the contact area of indentation, not the projected area. Therefore, H_V and P_m are related by

$$H_V = 0.927P_m \tag{6}$$

Eqs. (5.a) and (6) can be combined to obtain

$$\sigma_Y = \frac{H_V}{0.927C} \tag{7}$$

Taking $C=2.956$, H_V (MPa) versus σ_Y (MPa) plots can be expected to have a slope of 0.365 (3.580 when H_V is given in kg/mm^2) and the best fit lines should go through the origin. However, research on steels [14,23–26], magnesium [27], and aluminum [13,28] showed that the relationship between Vickers hardness and tensile yield stress is better expressed in the form

$$\sigma_Y = \beta_1 H_V + \beta_0 \tag{8}$$

In steels, the slope in Eq. (8), β_1, was found [24] to change between 0.268 and 0.390. In all studies, the y-intercept, β_0, was found to be negative. To the authors' knowledge, the consistent presence of a y-intercept that is different from zero has not been fully addressed in the literature. That is why some researchers [24,26] have chosen to report their findings in terms of $\Delta\sigma_Y/\Delta H_V$ (β_1).

Estimating tensile strength from hardness data has been mostly empirical in nature because the phenomenon of tensile instability after which engineering stress decreases with increased engineering strain does not occur during indentation. Based on data published in the literature, Zhang et al. [12] made the observation that for most carbon and alloy steels with different thermal treatments, S_T is approximately $H_V/3$, which if plotted against one another respectively would produce a slope of 0.333. This slope is similar to the one found (0.312) by Arptin and Murphy [29] for metals with $E \approx 70$ GPa, such as aluminum.

Although estimating σ_Y and S_T directly from the correlation with hardness has been viewed as a practical method [26], most research efforts have focused on the two other methods. Moreover, the discrepancy between the theoretical values based on contact mechanics and the best-fit equations to experimental data has not been addressed in detail. This study is intended to fill this gap in the literature.

3. Experimental details

A rectilinear open die forging of 7010 alloy was manufactured by HDA Forgings Ltd. (now Mettis Aerospace, Ltd.), Redditch, UK on a 20 MN draw down hydraulic press. The forging temperature was in the range 390–400 °C. This forging was similar to a production item that receives extensive machining and ultimately forms part of the wing spar assembly in the Airbus A330/A340. The rectilinear forging had dimensions of 3045 mm (L, longitudinal) × 158 mm (LT, long transverse) × 125 mm (ST, short transverse). The chemical composition of the forging is given in Table 1. Tensile specimens with 6 mm diameter and 30 mm gage length were excised from the forging. The long axis of the specimens corresponded to the L direction of the forging. Specimens were solution treated in an air-recirculating furnace at 475 °C for 50 min. Solution treatment was followed by 32 different quench paths, both interrupted and delayed quench [30] to obtain a wide interval of yield strength and hardness values. Quenches were interrupted at seven temperatures for various durations by inserting specimens into a salt bath filled with a eutectic mixture of KNO_3 and $NaNO_2$. In delayed quench experiments, specimens were initially cooled in still air until the target temperatures (400, 350, 300, 250, and 200 °C) were reached, and subsequently quenched in cold water. For each interrupted and delayed quench path, two tensile specimens were used. In addition, two specimens were quenched directly in cold water from the solution treatment temperature. Specimens were then naturally aged at room temperature for 5 days. Subsequently they were artificially aged at two stages, 120 °C for 10 h followed by 173 °C for 8 h, to attain the overaged condition.

Tensile and Vickers hardness tests were conducted on each specimen. A Zwick tensile tester was used at an engineering strain rate of 0.001/s and σ_Y and S_T values were recorded. A total of sixty five tensile tests were conducted. Three Vickers hardness tests at 20 kg load were conducted on an Instron Wolpert 930 Tester machine. At least three indentations were made on each specimen and their average was taken as the representative hardness value.

The composition of the 7010 plate used in this investigation is also given in Table 1. The material was supplied as a rolled plate (3403 × 1320 × 157 mm), which was manufactured from cast slab. A number of cross sectional slices (5.0 mm thick) were cut from one end of the plate perpendicular to the rolling direction. Each slice was further cut into five strips of equal width, each representing a different depth through the plate thickness. Flat tensile test specimens were manufactured from the strips to the dimensional requirements of British Standard BS 4A-4. They had a gauge length of 50 mm, a minimum parallel length of 63 mm, a minimum transition radius of 25 mm, a width of 12.5 mm and a thickness of 3 mm. The tensile test specimens were solution tre-

[1] In this study, Vickers hardness is reported in MPa, which is found by multiplying the traditional Vickers number by the gravitational acceleration.

Table 1
Chemical composition (in wt%) of 7010 alloys used in this study.

	Si	Fe	Cu	Mg	Zn	Zr	Al
Forging	0.03	0.06	1.69	2.44	6.26	0.14	Balance
Plate	0.04	0.05	1.75	2.34	6.30	0.12	Balance

ated at 475 °C for 50 min in a Caltherm air circulating furnace, quenched in water (~ 22 °C) at a quenching rate of about 95 °C/s, and then chilled to −18 °C for subsequent treatments. Three different aging treatments were employed:

1. natural aging for different durations between 15 min and 386 h (W-temper);
2. natural aging for 16 days, artificial aging at 120 °C for 10 h followed by 172 °C for different durations ranging from 10 min to 8 h;
3. natural aging for 16 days, artificial aging at 120 °C for 10 h followed by 172 °C and overaging at 172 °C for different durations ranging from 1 h to 100 h.

The experimental matrix allowed a wide range of temper conditions to be obtained by varying the duration of natural aging, artificial aging and overaging. The hardness measurements of the specimens were performed on a surface polished to approximately 1.5 μm prior to the tensile tests. The hardness was measured by a Vickers HTM8313 hardness tester with a 5 kg load. The tensile tests were carried out using an Avery Denison testing machine, Model 6157, with a load capacity of 100 KN, according to British Standard B.S. EN 10002-1.

4. Results and discussion

The microstructure of the 7010 forgings and plate is presented in Fig. 1. Fig. 1a shows the presence of Fe-bearing coarse phases (constituents) on grain boundaries. However the number density of these coarse phases is small, due to the low Fe content (0.06 wt%) of the alloy. The microstructure for the 7010 plate can be seen in Fig. 1b. One can question whether general issues with these two products, specifically the heterogeneous grain distributions in forgings and changes in homogeneous deformation at the start and end of the rolled products, could introduce scatter into the experimental results. It should be noted that despite the difference in the scale of the microstructure, yield stress can be assumed to be unaffected, as it has been shown [31] that 7010 is insensitive to Hall–Petch effects over this grain size range, just like in other aluminum alloys [32].

The H_V–σ_Y relationship for both datasets is presented in Fig. 2. Note that the two datasets overlap each other almost completely. Because the variation in properties was obtained by different quench paths and by different aging treatments for the forging and plate specimens, respectively, the overlap in Fig. 2 may not be coincidental and requires further theoretical analysis.

The estimated coefficients, β_1 and β_0, for the best fit line are provided in Table 2. Note that the slope of 0.365 expected from Tabor's analysis is not within the 95% confidence interval for β_1. Therefore the common assumption that $\Delta P_m/\Delta\sigma_Y=3$ is not valid for 7010.

Shaw and DeSalvo [33], in their analysis for a blunt axisymmetric indenter, found that the constraint factor, C, is 2.82. This value is very similar to the one found by Shield [34] ($C=2.84$) for a round punch pushing against a deforming metal. Moreover, $C=2.82$ is essentially the same as the constraint factors that Tabor [22] reported for copper and mild steel. Larsson [35] reported $C=2.80$ in his study of Vickers hardness test by finite element modeling. Inserting

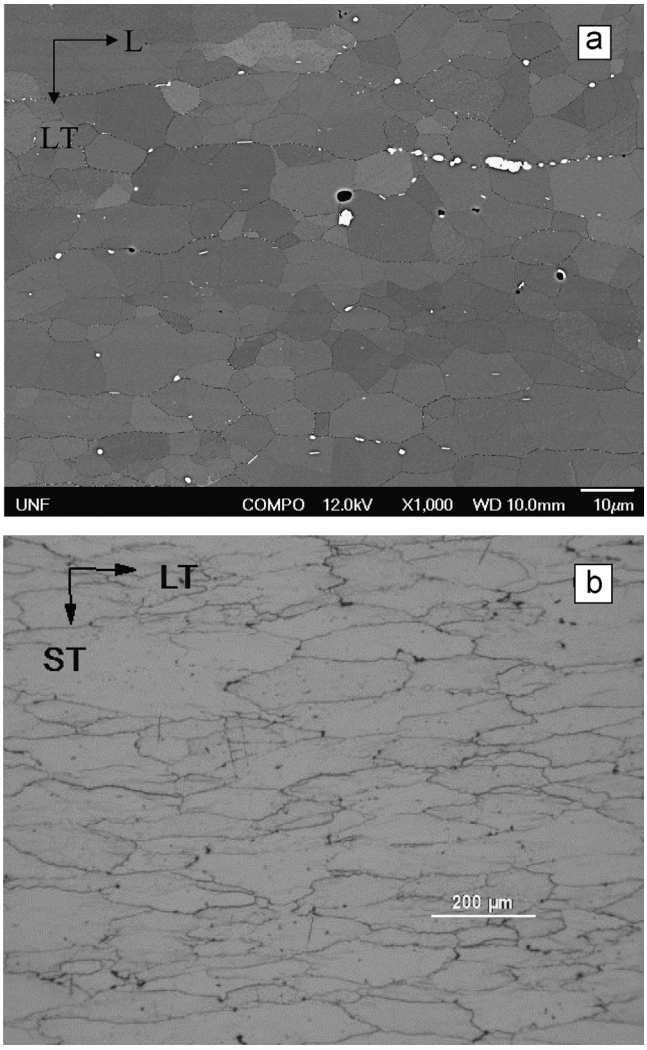

Fig. 1. The typical microstructure of the 7010 alloy: (a) SEM image of specimen from forging at low magnification, demonstrating grain size and coarse constituents common to the samples in this study. Long axis of the photograph corresponds to the longitudinal axis of the tensile specimens and the original forging. The microstructure of rolled plate is given in the optical micrograph in (b).

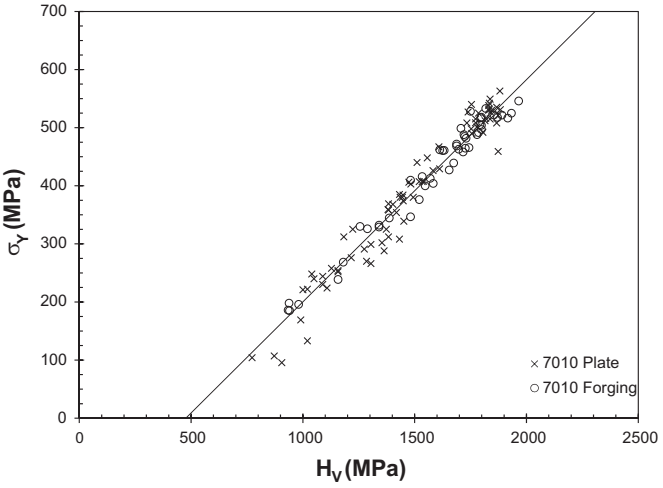

Fig. 2. Vickers hardness versus yield stress for 7010 plate and forging investigated in this study. The line is obtained by Eq. (8.a).

$C=2.82$ into Eq. (7), the slope ($\Delta\sigma_Y/\Delta H_V$) is calculated as 0.383 (3.752 when H_V is in kg/mm^2). This slope is very close to the one obtained by linear regression and is within the 95% confidence

Table 2
Results of linear regression analyses.

	β_1			β_0 (MPa)			R^2
	Estimate	95% lower	95% upper	Estimate	95% lower	95% upper	
σ_Y (MPa)	0.391	0.376	0.406	−195.7	−218.6	−172.7	0.958
S_T (MPa)	0.247	0.237	0.257	113.1	98.1	128.2	0.954

interval given in Table 2. Hence, the fit was recalculated by holding the slope constant at 0.383;

$$\sigma_Y = 0.383H_V - 182.3 \quad (8.a)$$

The coefficient of determination, R^2, for Eq. (8.a) is 0.957 which is almost identical to the R^2 obtained by linear regression given in Table 2. The line in Fig. 2 is drawn by using Eq. (8.a). If the line obtained by regression were drawn in Fig. 2, it would almost completely overlap the line obtained by Eq. (8.a). Therefore, it is recommended that $\Delta\sigma_Y/\Delta H_V$ be taken as 0.383 for 7010.

To check for further consistency, the data from a third independent quench sensitivity study by Flynn [36,37] for a 7010 aluminum alloy forging were used and fitted with Eq. (8.a). The results are presented in Fig. 3. Despite more scatter in this dataset, it is remarkable that the same equation provided such a respectable fit to Flynn's data, with $R^2=0.874$.

Table 2 shows the 95% confidence interval for the y-intercept, β_0. Because zero is not within the confidence limits, there is very strong evidence that the best fit line cannot go through the origin, a result consistent with previous studies. It should be mentioned that Vickers hardness test is designed to generate a constant characteristics strain under the indenter. This characteristic strain was stated as 8% by Tabor [3] and 7% by Johnson [38]. In fully work-hardened materials, stress increases elastically to yield stress after which it remains constant despite increasing strain (full plasticity). In many early studies on the hardness of metals, the materials were specifically chosen to be fully work-hardened, ensuring that flow stress was equal to yield stress so that stress calculations always resulted in an estimate of the yield stress. In metals that are not yet fully work hardened, the effect of work hardening that occurs during indentation must be accounted for. The calculation of stress under the indenter leads to the estimate of the flow stress at the corresponding strain. Hence, Eq. (7) can be written in a more generalized form;

$$\sigma_f = \frac{H_V}{0.927C} \quad (7.a)$$

Consequently, in a Vickers hardness test on a metal that has not fully work-hardened, $\sigma_f > \sigma_Y$. The stress generated under the Vickers indenter in a work-hardening metal can be represented as

$$\sigma_f = \sigma_Y + \Delta\sigma \quad (9)$$

where $\Delta\sigma$ is the increase in stress due to work hardening during deformation to 8% characteristic strain. Obviously, for fully work-hardened metals, $\Delta\sigma=0$. After inserting Eq. (9) into Eq. (7) and rearranging, we obtain;

$$\sigma_Y = \frac{H_V}{0.927C} - \Delta\sigma \quad (10)$$

Eq. (10) helps explain why the y-intercept is consistently negative in previous studies for materials that work-harden during plastic deformation. Moreover, Eq. (10) is consistent with the model suggested by Larsson [35]. Further research is needed to investigate the effect of work hardening on Vickers-hardness–yield stress relationship among other structural and process variables.

Turning the attention to tensile strength, the relationship between Vickers hardness and tensile strength is presented in Fig. 4. Again, the results from two studies overlap significantly. In Fig. 4,

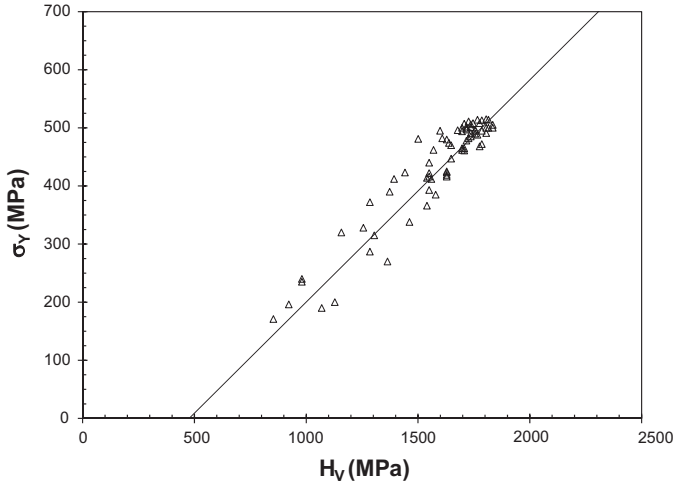

Fig. 3. Vickers hardness versus yield stress relationship drawn from the data of Flynn [36,37]. The line is obtained from Eq. (8.a), which provides an excellent fit to the data.

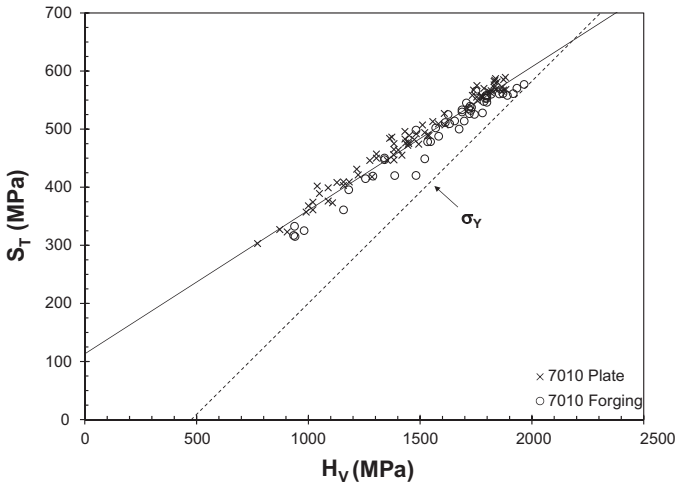

Fig. 4. Tensile strength versus Vickers hardness for 7010 plate and forging.

the best fit line has the following equation:

$$S_T = 0.247H_V + 113.1 \quad (11)$$

The coefficient of determination is quite respectable ($R^2=0.954$). The line for yield stress is also included in Fig. 4 for reference. The confidence intervals for the slope and the intercept for Eq. (1) are presented in Table 2.

The value of $\beta_1=0.247$ (2.423 when H_V is in kg/mm^2) is significantly different from 0.333 observed in steels, indicating a clear behavioral distinction between steels and the 7010 alloys in this study. However, it is unclear why the value of the slope found in this study is significantly different from the one reported by Arbtin and Murphy [29] for alloys with a modulus of elasticity similar to that of 7010. Additionally, zero is not within the 95% confidence interval for β_0, indicating a positive y-intercept. Because of the empirical nature of the H_V–S_T relationship, no further analysis has been conducted at this time.

5. Conclusions

1. The Vickers hardness–yield stress relationship in 7010 has been developed from two independent datasets:

$$\sigma_Y = 0.383H_V - 182.3$$

The slope of 0.383 is linked to contact mechanics principles reported in the literature. Specifically, the constraint factor of 2.82 was used in deriving the slope.

2. The negative *y*-intercept found in this study has been consistently reported in the literature. The reason for the negative intercept can be explained by the increase in stress under the indenter due to work hardening until it reaches the characteristic strain in Vickers hardness testing. While the model proposed is consistent with the analytical solution of Larsson, a phenomenological study is planned to investigate the effect of work hardening among other structural and process variables.
3. That data from two independent studies using the aluminum alloy 7010 overlapped is quite significant and indicates a fundamental relationship between hardness and strength. The same fit to both datasets also provided a very respectable fit to a third independent study.
4. An empirical relationship between tensile strength and Vickers hardness was also developed:

$$S_T = 0.247H_V + 113.1$$

5. This relationship is supported by overlapping data from two independent studies. The slope of 0.247 is significantly different from that reported in the literature for steels (0.333) and for nonferrous alloys with a modulus of elasticity similar to that of 7010 (0.312).

References

[1] R.R. Cervay, Mechanical Property Evaluation of Aluminum Alloy 7010-T73651, AFWAL-TR-80-4094, 1980.
[2] MIL-A-21180D, Military Specification Aluminum Alloy Castings, High Strength, U.S. Department of Defense, 1984.
[3] D. Tabor, The Hardness of Metals, Oxford, London, 1951.
[4] M. Tiryakioğlu, J. Campbell, Mater. Sci. Eng. A A361 (2003) 232–239.
[5] R. Hill, B. Storåkers, A.B. Zdunek, Proc. R. Soc. Lond. A436 (1989) 301–330.
[6] B. Taljat, T. Zacharia, F. Kosel, Int. J. Solids Struct. 35 (1998) 4411–4426.
[7] S.D. Mesarovic, N.A. Fleck, Proc. R. Soc. Lond. A 455 (1999) 2707–2728.
[8] A.E. Giannakopoulos, S. Suresh, Scr. Mater. 40 (1999) 1191–1198.
[9] A.E. Giannakopoulos, P.-L. Larsson, R. Vestergaard, Int. J. Solids Struct. 31 (1994) 2679–2708.
[10] J.M. Antunes, L.F. Menezes, J.V. Fernandes, Int. J. Solids Struct. 43 (2006) 784–806.
[11] M. Tiryakioğlu, J. Campbell, J.T. Staley, Mater. Sci. Eng. A 361 (2003) 240–248.
[12] P. Zhang, S.X. Li, Z.F. Zhang, Mater. Sci. Eng. A 529 (2011) 62–73.
[13] M.A. Salazar-Guapuriche, Y.Y. Zhao, A. Pitman, A. Greene, Mater. Sci. Forum 519–521 (2006) 853–858.
[14] E.J. Pavlina, C.J. Van Tyne, J. Mater. Eng. Perform. 17 (2008) 888–893.
[15] R.A. George, S. Dinda, A.S. Kasper, Met. Prog. (1976) 30–35.
[16] B.S. Shabel, R.F. Young, Light Met. Age 45 (5–6) (1987) 28–31.
[17] Y.T. Cheng, C.M. Cheng, Mater. Sci. Eng. R 44 (2004) 91–149.
[18] M. Tiryakioğlu, J.S. Robinson, P.D. Eason, Mater. Sci. Eng. A 618 (2014) 22–28.
[19] M.A. Salazar-Guapuriche, Evolution of Electrical Conductivity, Hardness and Strength during Age Hardening of AA7010 (Ph.D. thesis), University of Liverpool, 2009.
[20] E. Meyer, Z. Ver. Deutsch. Ing. 52 (1908) 645–654.
[21] R. Hill, E.H. Lee, S.J. Tupper, Proc. R. Soc. Lond. Ser. A 188 (1947) 273–289.
[22] D. Tabor, Proc. R. Soc. Lond. Ser. A 192 (1948) 247–274.
[23] H.R. Higgy, F.H. Hammad, J. Nucl. Mater. 55 (1975) 177–186.
[24] J.T. Busby, M.C. Hash, G.S. Was, J. Nucl. Mater. 336 (2005) 267–278.
[25] O. Takakuwa, Y. Kawaragi, H. Soyama, J. Surf. Eng. Mater. Adv. Technol. 3 (2013) 262–268.
[26] M.O. Lai, K.B. Lim, J. Mater. Sci. 26 (1991) 2031–2036.
[27] C.H. Caceres, J.R. Griffiths, A.R. Pakdel, C.J. Davidson, Mater. Sci. Eng. A 402 (2005) 258–268.
[28] S. Sato, Kei Kinzoku Yosetsu 35 (1997) 21–30.
[29] E. Arbtin, Jr., G. Murphy, Correlation of Vickers Hardness Number Modulus of Elasticity and the Yield Strength for Ductile Metals, Report no: ISC-356, Ames Laboratory, US Atomic Energy Commission, 1953.
[30] W.L. Fink, L.A. Willey, Trans. AIME 175 (1948) 414–427.
[31] J. Campbell, Complete Casting Handbook, Elsevier, London (2011) 543.
[32] J.D. Embury, D.J. Lloyd, T.R. Ramachandran, Strengthening Mechanisms in Aluminum Alloys, Treatise on Materials Science and Technology, vol. 31, Academic Press, London (1989) 579–601.
[33] M.C. Shaw, G.J. DeSalvo, Trans. ASME: J. Eng. Ind. 92 (1970) 480–494.
[34] R.T. Shield, Proc. R. Soc. Lond. A 233 (1955) 267–287.
[35] P.-L. Larsson, Intl. J. Mech. Sci. 43 (2001) 895–920.
[36] R.J. Flynn, J.S. Robinson, J. Mater. Process. Technol. 153–154 (2004) 674–680.
[37] R.J. Flynn, Property Prediction and Residual Stresses in Aluminium Alloy 7010 (Ph.D. thesis), University of Limerick, Ireland, 2013.
[38] K.L. Johnson, Contact Mechanics, Cambridge University Press, New York, 1985.